



Kahramanmaraş Sütçü İmam University

Journal of Engineering Sciences



Geliş Tarihi : 02.10.2023
Kabul Tarihi : 28.12.2023

Received Date : 02.10.2023
Accepted Date : 28.12.2023

A NOVEL STUDY ON THE SYNTHESIS, CHARACTERIZATION, AND PHOTOCATALYTIC ACTIVITY OF CeO₂ NANOPARTICLES

CeO₂ NANOTANECİKLERİNİN SENTEZİ, KARAKTERİZASYONU VE FOTOKATALİTİK AKTİVİTESİ

Nazlı TURKTEN^{1*} (ORCID: 0000-0001-9343-3697)

Yunus KARATAS¹ (ORCID: 0000-0002-3826-463X)

¹ Department of Chemistry, Faculty of Arts and Sciences, Kirsehir Ahi Evran University, Kirsehir, 40100, Türkiye

*Sorumlu Yazar / Corresponding Author: Nazlı TURKTEN, nazli.turkten@yahoo.com

ABSTRACT

The discharge of untreated wastewater from unplanned industrial activities using dyes can cause serious environmental pollution and affect the aquatic environment. Semiconductor photocatalysis is a favorable technology widely used for degrading organic dyes in wastewater. This study dealt with the preparation of CeO₂ nanoparticles via a simple precipitation technique. Information on the structural and morphological features of the developed CeO₂ nanoparticles were determined using Fourier transform infrared with attenuated total reflectance (FTIR-ATR), Raman spectroscopy, X-ray diffraction (XRD), and scanning electron microscopy (SEM) spectroscopic methods. The presence of the characteristic bands of CeO₂ in the FTIR spectrum provided evidence of successful CeO₂ formation. The calculated crystallite particle size utilizing the Scherrer equation was 10 nm. SEM images revealed that the morphology of CeO₂ consisted of almost spherical particles with slight agglomeration. Brunauer-Emmett-Teller (BET) technique was also used to find out the specific surface area of CeO₂ nanoparticles (11 m²/g). The efficiency of CeO₂ nanoparticles was also confirmed in terms of their photocatalytic activity against Rhodamine B (Rh B) under UV-A light. The results indicated that CeO₂ nanoparticles could be a promising catalyst candidate for industrial wastewater treatment.

Keywords: CeO₂ nanoparticles, photocatalyst, photocatalysis, Rhodamine B, wastewater treatment.

ÖZET

Boya içeren endüstriyel atık suyunun yeterli bir arıtma işlemi yapılmadan boşaltılması sonucunda önemli çevre ve su kirliliği oluşabilir. Yarı iletken fotokataliz, atık sulardaki organik boyaların parçalanması amacıyla yaygın olarak kullanılan uygun bir teknolojidir. Bu çalışmada, CeO₂ nanotanecikleri basit bir çöktürme yöntemi kullanılarak hazırlanmıştır. Fourier dönüşümlü kızılötesi spektroskopisi-zayıflatılmış toplam yansıma (FTIR-ATR), Raman spektroskopisi, X-ışını difraktometresi (XRD) ve taramalı elektron mikroskopu (SEM) yöntemleri kullanılarak CeO₂ nanotaneciklerinin yapısal ve morfolojik özellikleri belirlenmiştir. FTIR spektrumunda yer alan karakteristik bandların varlığı CeO₂ oluşumunun başarılı bir şekilde gerçekleştiğini göstermiştir. Scherrer eşitliği kullanılarak kristal tanecik boyutu 10 nm olarak hesaplanmıştır. SEM görüntüleri, CeO₂'nin morfolojisinin yüzeyde çok az bir toplanma olsa da neredeyse küresel taneciklerden oluştuğunu ortaya çıkarmıştır. Brunauer-Emmett-Teller (BET) yöntemi kullanılarak CeO₂ nanotaneciklerinin spesifik yüzey alanı (11 m²/g) belirlenmiştir. CeO₂ nanotaneciklerinin etkinliği, UV ışığı altında Rhodamin B (Rh B) boyasına karşı fotokatalitik aktiviteleri incelenerek saptanmıştır. Elde edilen sonuçlar, CeO₂ nanotaneciklerinin endüstriyel atıksu arıtımında kullanılabilecek, ileriye dönük ümit vaat eden bir katalizör olduğunu göstermiştir.

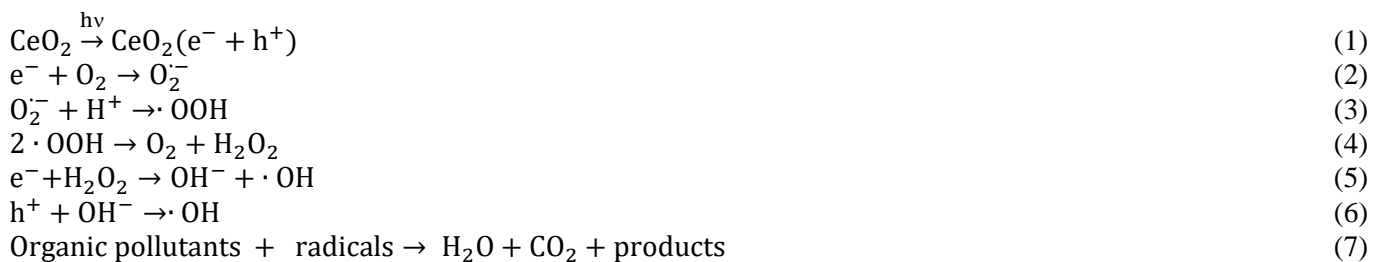
Anahtar Kelimeler: CeO₂ nanotanecikleri, fotokatalizör, fotokataliz, Rhodamin B, atıksu arıtımı.

INTRODUCTION

Unauthorized industrial wastewater discharge containing dyes from textiles, printing, paper, and food processing is a currently growing pollution problem that can cause adverse environmental and health problems (Soleyman et al., 2023). The textile industry is known to be one of the largest consumers of dyes, resulting in excessive amounts of wastewater containing dye effluents (Amalina et al., 2022; Sharma & Soni, 2021). Rh B is widely used as a water-soluble textile dye colorant with carcinogenic and neurotoxic effects that can cause an extremely toxic value in textile wastewater (Al-Buriah et al., 2022; Al-Gheethi et al., 2022).

The significance of developing efficient and modern water treatment methods has become an urgent task to prevent the negative impact of the widespread distribution of Rh B contaminated, incompletely treated wastewater into water bodies and thus to ensure the safe disposal of dye effluents in aquatic environments (Al-Buriah et al., 2022; Linghu et al., 2023; Ma et al., 2021; Soleyman et al., 2023). Despite global efforts to address this challenging issue, traditional approaches are still inadequate and have many disadvantages. Physical methods are insufficient for the complete removal of organics from wastewater. Biological treatment techniques are expensive and require long preparation cycles. On the other hand, advanced oxidation processes (AOPs) are applied as a highly effective chemical method that can degrade organics entirely with a rapid oxidation rate. The most commonly used AOPs are photocatalytic oxidation, Fenton reactions, and electrochemical oxidation reactions that do not cause secondary pollution (Ma et al., 2021; Soleyman et al., 2023). Among the AOPs, photocatalysis has proven to be fast, low operating cost, chemical free, environmentally friendly, highly stable, and has high removal efficiency for recalcitrant contaminants from water. In photocatalysis, reactive oxygen species (ROS) are produced during oxidation processes when a semiconductor is captured by light (Durodola et al., 2023; Soleyman et al., 2023).

Ceria, also known as CeO₂, plays a key role in a diversity of applications, particularly in optical devices, solar cells, fuel oxidation catalysis, photocatalysis, and the biological field, as this n-type semiconductor has a unique crystal structure and electronic features (Ma et al., 2023; Pansambal et al., 2022). Today, CeO₂ nanoparticles are considered as one of the most promising catalyst candidates, showing encouraging results in wastewater treatment technologies as well as photocatalysis (Kurian, 2020; Kusmierk, 2020). The exceptional characteristics and superior properties of CeO₂ are being non-toxic, inexpensive, having high chemical stability, and an efficient oxygen storage capability that makes this semiconductor as a pivotal importance photocatalyst (Tran et al., 2022). The reaction Equations (1-7) corresponding to the photocatalytic degradation mechanism of organic pollutants using CeO₂ are given as follows (Ma et al., 2019):



The photocatalytic degradation mechanism of CeO₂ begins with the irradiation of light on the semiconductor surface ($>E_g$), resulting in electron excitation followed by a photogeneration process to produce electron/hole (e^-/h^+) pairs. These charge carriers produced in the photocatalyst are forwarded to redox reactions to form ROS containing superoxide and hydroxyl radicals as represented in the equations. Highly oxidizing hydroxyl radicals attack organic pollutants forming products as well as converting them into harmless compounds such as CO₂ and H₂O via a complete mineralization (Ma et al., 2019).

The present study reported the preparation of CeO₂ nanoparticles using a simple precipitation route that could provide broad possible aspects in wastewater treatment. FTIR-ATR, Raman spectroscopy, XRD analysis were utilized to confirm the structural properties of CeO₂ nanoparticles and the morphology of CeO₂ was investigated by SEM analysis. BET method and BJH pore size distribution technique were applied to identify the surface properties of CeO₂. Furthermore, the photocatalytic application of CeO₂ nanoparticles in the photodegradation of Rh B dye under UV light irradiation was investigated.

MATERIALS AND METHODS

Materials

Ammonium cerium (IV) nitrate ($\text{Ce}(\text{NH}_4)_2(\text{NO}_3)_6$), Sigma-Aldrich, ACS reagent, $\geq 98.5\%$) and sodium hydroxide (NaOH, Sigma-Aldrich, ACS reagent, $\geq 97.0\%$, pellets) were used without further purification. Distilled water was used for the preparation of all solutions used in experiments.

Preparation of CeO_2 Nanoparticles

CeO_2 nanoparticles were synthesized via a modified precipitation method (Seeharaj et al., 2019). In the usual synthesis procedure, 100 mL of 0.1 M $\text{Ce}(\text{NH}_4)_2(\text{NO}_3)_6$ solution was placed in a flat bottomed flask. 0.5 M NaOH solution was used to adjust the pH=12 and then added dropwise to $\text{Ce}(\text{NH}_4)_2(\text{NO}_3)_6$ solution under vigorous stirring. The entire solution continued stirring well for 2 h. The solution was then filtered, washed with distilled water, and dried in an oven at 80°C for 24 h. The pale-yellow CeO_2 nanoparticles were calcinated for 2 h using a porcelain crucible at 500°C .

Characterization Techniques

FTIR-ATR measurements (Perkin Elmer Spectrum Two) were acquired at a resolution of 4 cm^{-1} in the range of $2000\text{--}400\text{ cm}^{-1}$. Dispersive Raman spectroscopy (Thermo Scientific DXR Raman Microscope) was performed using an Ar^+ laser excitation at $\lambda=532\text{ nm}$ with an applied power of 10 mW. SEM analysis (FEI-Philips XL30 Scanning Electron Microscope) was carried out with an operational accelerating voltage of 10 kV. XRD diffractograms (Rigaku-D/MAX-Ultima diffractometer) were obtained using $\text{Cu K}\alpha$ radiation ($\lambda=1.54\text{ \AA}$) with operational parameters of 40 kV and 40 mA. BET technique and BJH pore size distribution model were used on a Quantachrome Quadrosorb SI instrument. The analytical procedure applied for nitrogen isotherm tests was at 77 K.

Photocatalytic Activity Assessment

Photocatalytic activity experiments were performed in a Pyrex vessel illuminated using a black light fluorescent lamp (125 W) placed at the top of the reactor. The volume of the solution in photocatalytic activity test was 50 mL containing a concentration of Rh B solution (10 mg/L) with a dose of CeO_2 nanoparticles (0.25 g/L). The absorption changes of Rh B dye at maximum absorbance wavelength ($\lambda_{\text{max}}=553\text{ nm}$) were monitored using a UV-vis spectrophotometer. Additional detailed information on the photocatalytic system was reported in our previous work (Turkten, 2022).

RESULTS AND DISCUSSION

Characterization of CeO_2 nanoparticles

The surface functional groups and chemical bonding of CeO_2 nanoparticles were proved by FTIR-ATR spectroscopy and the results were presented in Figure 1. The intense band observed at 1341 cm^{-1} was attributed to the stretching mode of vibration $\nu(\text{Ce-O-Ce})$ while the band at 467 cm^{-1} corresponded to the stretching $\nu(-\text{Ce-O})$ vibration bond in CeO_2 . Moreover, a small band at 587 cm^{-1} could be assigned to the stretching $\nu(\text{O-Ce-O})$ vibrational signal. The small bands located at 1042 cm^{-1} and 834 cm^{-1} belong to the stretching vibration of $\nu(\text{NO}_3^-)$ indicating the existence of residual nitrate moiety (Ramadan & El-Masry, 2021; Turkten, 2022; Vivek & Babu, 2016; Xie et al., 2021).

The Raman spectrum of CeO_2 nanoparticles revealed a major band at 458 cm^{-1} and a small band at 585 cm^{-1} corresponding to F_{2g} mode and LO mode, respectively (Figure 2). The F_{2g} mode was related to the fluorite structure, addressing the symmetrical stretching of oxygen around each cerium, while the non-degenerate LO mode belonged to the O^{2-} vacancies resulting from nonstoichiometric oxygen vacancies in CeO_2 (Babitha et al., 2014; Malleshappa et al., 2016).

The XRD diffractogram of CeO_2 nanoparticles was revealed in Figure 3. The specific diffraction peaks are indexed on the standard card JCPDS NO. 43-1002. The diffraction angles, $2\theta = 28.54^\circ, 33.26^\circ, 47.58^\circ, 56.52^\circ, 59.32^\circ, 69.72^\circ, 76.64^\circ, \text{ and } 79.08^\circ$ corresponded to (111), (200), (220), (311), (222), (400), (331), and (420) planes of pure CeO_2 . The XRD diffractogram of CeO_2 nanoparticles agreed with the ideal fluorite lattice position related to the (111) plane located at $2\theta = 28.54^\circ$ (Cerrato et al., 2022; Chang et al., 2022). The XRD analysis was also well-matched with the fluorite-type structure of CeO_2 , as confirmed by Raman data.

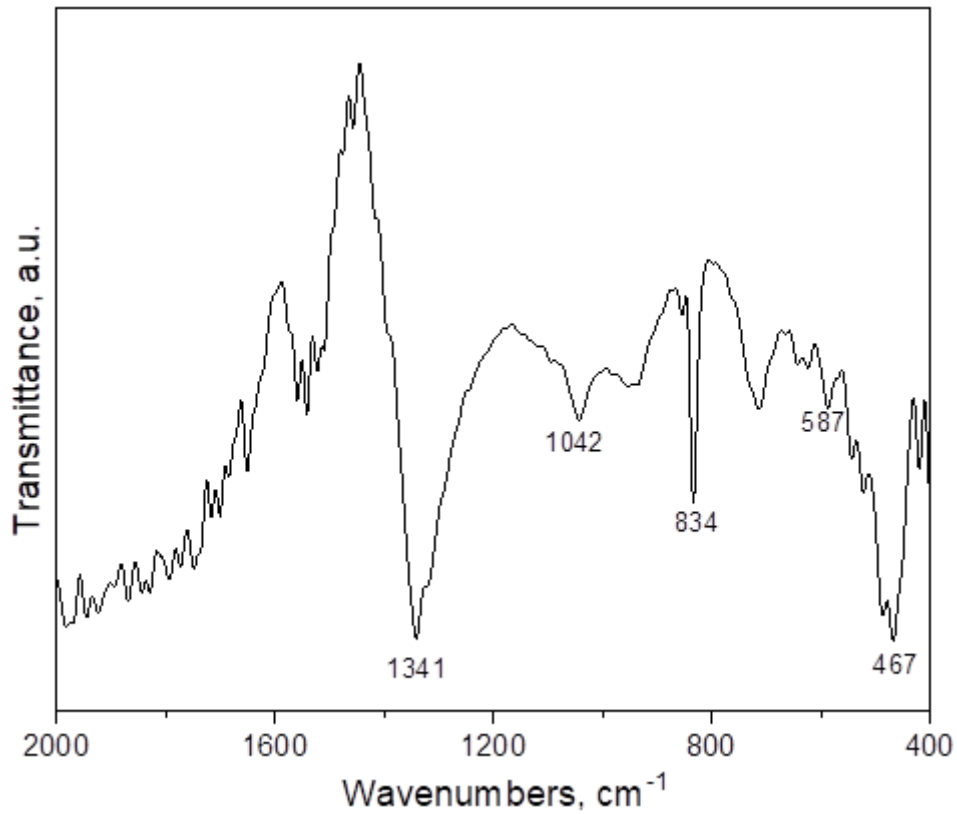


Figure 1. FTIR-ATR Spectrum of CeO₂ Nanoparticles.

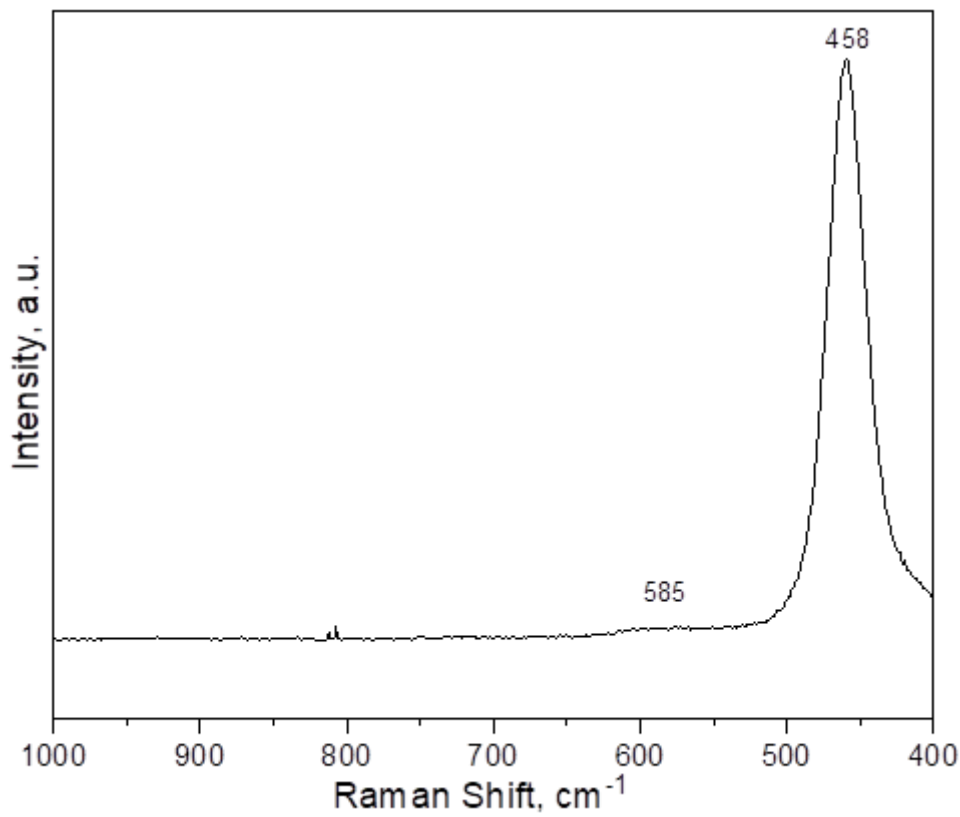


Figure 2. Raman Spectrum of CeO₂ Nanoparticles.

The crystallite size (D , nm) of CeO_2 nanoparticles was estimated from the (111) plane of CeO_2 by according to the Scherrer formula (Equation (8)) (Scherrer, 1918).

$$D = K \lambda / (\beta \cos\theta) \quad (8)$$

In Equation (8), $K = 0.9$, $\lambda = 1.5418 \text{ \AA}$, θ is the Bragg angle, and β is the full width at half maximum intensity. The calculated crystallite size of CeO_2 particles was 10 nm, therefore CeO_2 particles were designated as CeO_2 nanoparticles throughout the manuscript.

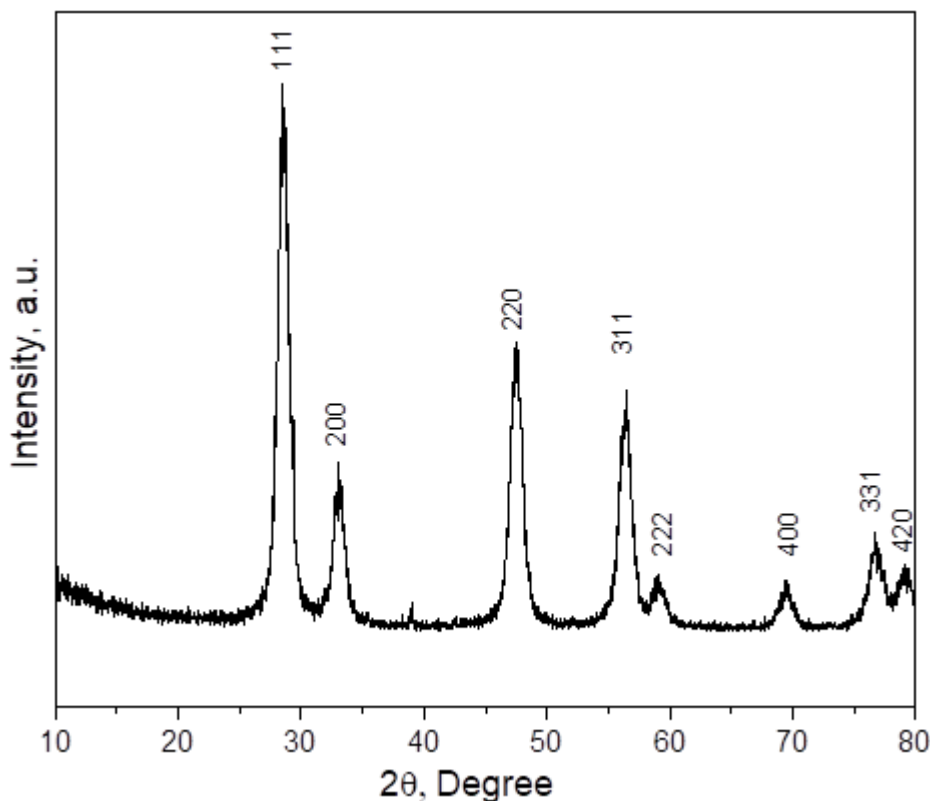


Figure 3. XRD Spectrum of CeO_2 Nanoparticles.

The surface morphological properties of CeO_2 nanoparticles were examined by SEM analysis (Figure 4). SEM images of CeO_2 nanoparticles revealed almost spherical particles with a slight agglomeration (Figure 4 (a)). The particle size was about 15 nm in diameter. The influence of pores on the CeO_2 surface with a few aggregates was clearly seen in Figure 4 (b).

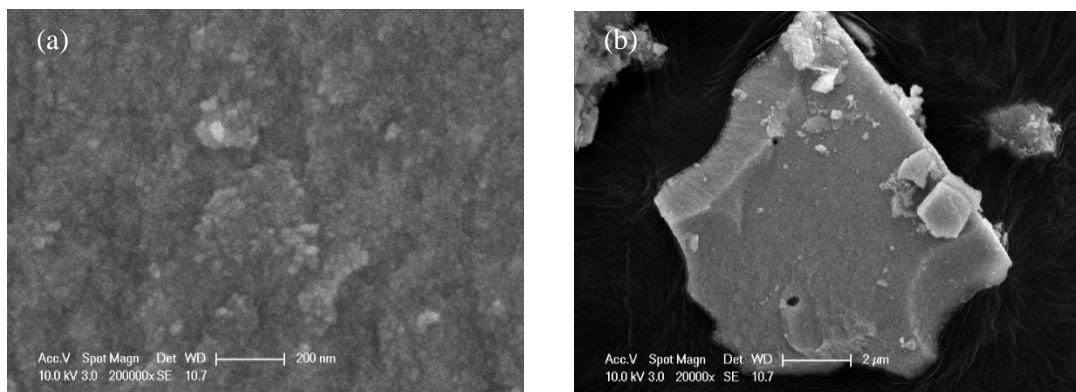


Figure 4. SEM Images of CeO_2 Nanoparticles (a) 200000x, (b) 20000x.

The calculated BET specific surface area of CeO_2 nanoparticles was $11 \text{ m}^2/\text{g}$. This value was in agreement with the experimental BET surface areas reported in the literature (De Faria & Trasatti, 1994). The pore size diameter obtained

from BJH method was 2.51 nm, which was in agreement with the pore size distribution between 2 nm and 50 nm, indicating a mesoporous character (Sing, 1985).

Photocatalytic activity

The photocatalytic degradation ability of Rh B using CeO₂ nanoparticles over an irradiation time of 60 min to 300 min was presented in Figure 5. Moreover, the degree of Rh B decolorization by using CeO₂ nanoparticles was also estimated by the following (Equation (9)):

$$\text{Decolorization, \%} = ((A_{553,0} - A_{553}) / A_{553,0}) \times 100 \tag{9}$$

where,

A_{553,0}: initial absorbance of Rh B dye,

A₅₅₃: absorbance of Rh B dye irradiated time at t.

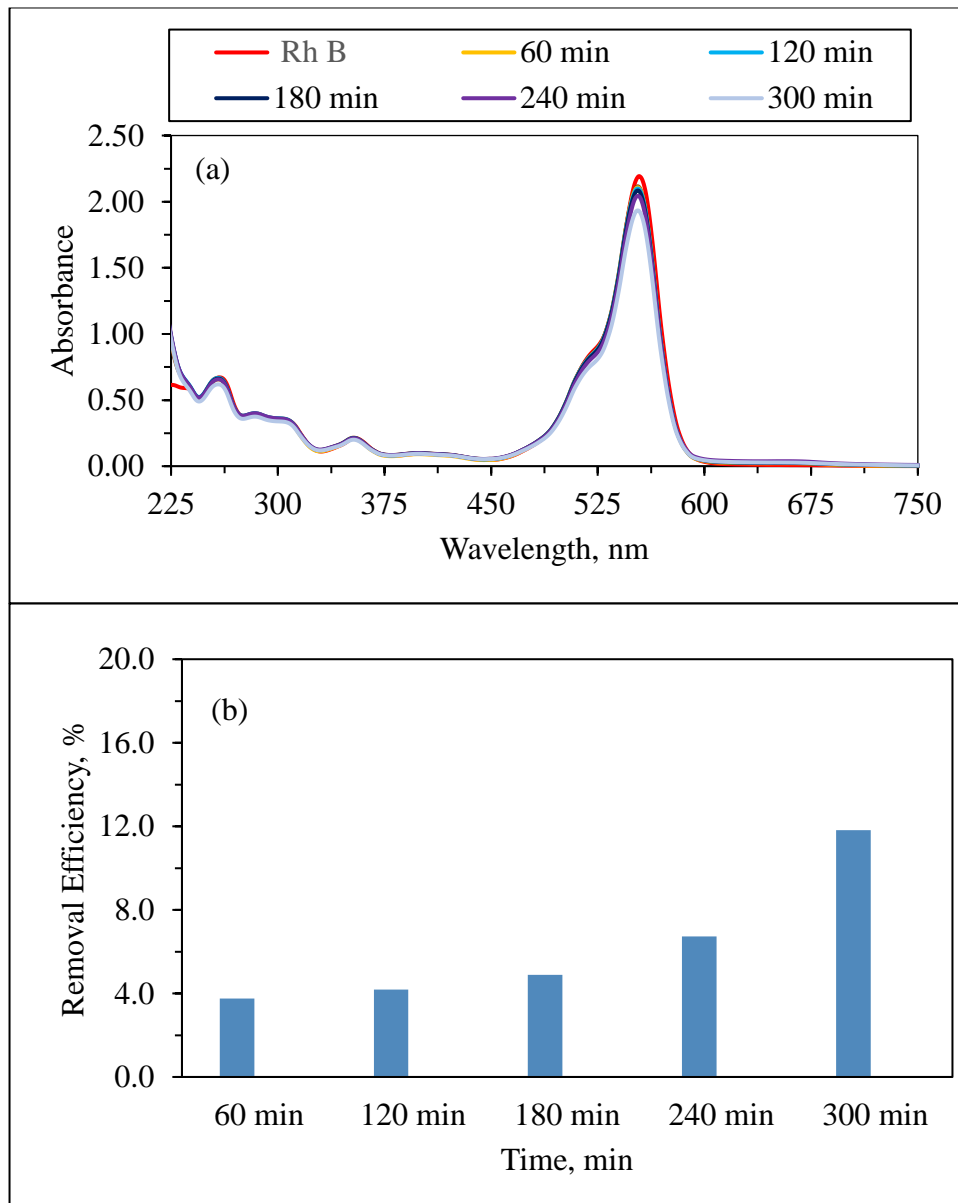


Figure 5. (a) UV-vis Photocatalytic Degradation Profiles of CeO₂ nanoparticles, (b) Photocatalytic Decolorization Degree of Rh B upon the Presence of CeO₂ Nanoparticles.

The observed reduction in the maximum wavelength absorption peak ($\lambda_{\max}=553$ nm) with time could indicate the destruction of the conjugated xanthene structure of Rh B and the photocatalytic degradation of dye (Hu et al., 2015). The Rh B removal decolorization degree of the CeO₂ nanoparticles was maintained at 12% after 300 minutes of irradiation. This slow degradation could be explained by the surface charges of both CeO₂ nanoparticles and Rh B. It was reported that the isoelectric potential of CeO₂ was pH=6-8-7.3 (Issarapanacheewin et al., 2016; Nadjia, et al., 2018; Wu et al., 2021). The pH of the solution used in this photocatalytic study was at around pH=6.0. Since the surface of CeO₂ was positively charged at this pH value, Rh B cationic dye molecules were preferably repelled from the CeO₂ surface. This repulsion could result in a low decolorization degree of Rh B.

CONCLUSION

In this study, CeO₂ nanoparticles were synthesized in a cost-effective and facile way by precipitation method. Structural and morphological properties of CeO₂ nanoparticles were confirmed by FTIR-ATR, Raman, XRD, and SEM analysis. XRD and Raman results indicated a fluorite structure of CeO₂. The functional groups of CeO₂ were verified from FTIR-ATR results. SEM images revealed that CeO₂ nanoparticles exhibited almost spherical particles with slight agglomeration. Rh B was chosen as the cationic model dye, and the photocatalytic degradation of Rh B upon the use of CeO₂ nanoparticles was also investigated. Henceforth, future photocatalytic studies on anionic dye removal are proposed for prospects in research, with an overall benefit for a further application of CeO₂ nanoparticles used in the field of catalysis. The prepared CeO₂ nanoparticles could be a promising candidate material that could be utilized for various applications, especially in photocatalysis, solar cell, and optoelectronics.

REFERENCES

- Al-Buriah, A. K., Al-Gheethi, A. A., Senthil Kumar, P., Radin Mohamed, R. M. S., Yusof, H., Alshalif, A. F., & Khalifa, N. A. (2022). Elimination of rhodamine B from textile wastewater using nanoparticle photocatalysts: A review for sustainable approaches. *Chemosphere*, 287, 132162. doi:https://doi.org/10.1016/j.chemosphere.2021.132162
- Al-Gheethi, A. A., Azhar, Q. M., Senthil Kumar, P., Yusuf, A. A., Al-Buriah, A. K., Radin Mohamed, R. M. S., & Al-shaibani, M. M. (2022). Sustainable approaches for removing Rhodamine B dye using agricultural waste adsorbents: A review. *Chemosphere*, 287, 132080. doi:https://doi.org/10.1016/j.chemosphere.2021.132080
- Amalina, F., Abd Razak, A. S., Krishnan, S., Zularisam, A. W., & Nasrullah, M. (2022). A review of eco-sustainable techniques for the removal of Rhodamine B dye utilizing biomass residue adsorbents. *Physics and Chemistry of the Earth, Parts A/B/C*, 128, 103267. doi:https://doi.org/10.1016/j.pce.2022.103267
- Babitha, K. K., Priyanka, K. P., Sreedevi, A., Ganesh, S., & Varghese, T. (2014). Effect of 8MeV electron beam irradiation on the structural and optical properties of CeO₂ nanoparticles. *Materials Characterization*, 98, 222-227. doi:https://doi.org/10.1016/j.matchar.2014.11.004
- Cerrato, E., Calza, P., & Cristina Paganini, M. (2022). Photocatalytic reductive and oxidative ability study of pristine ZnO and CeO₂-ZnO heterojunction impregnated with Cu₂O. *Journal of Photochemistry and Photobiology A: Chemistry*, 427, 113775. doi:https://doi.org/10.1016/j.jphotochem.2022.113775
- Chang, S., Jia, Y., Zeng, Y., Qian, F., Guo, L., Wu, S., Lu, J., & Han, Y. (2022). Effect of interaction between different CeO₂ plane and platinum nanoparticles on catalytic activity of Pt/CeO₂ in toluene oxidation. *Journal of Rare Earths*, 40(11), 1743-1750. doi:https://doi.org/10.1016/j.jre.2021.10.009
- De Faria, L. A., & Trasatti, S. (1994). The point of zero charge of CeO₂. *Journal of Colloid and Interface Science*, 167(2), 352-357. doi:https://doi.org/10.1006/jcis.1994.1370
- Durodola, S. S., Akeremale, O. K., Ore, O. T., Bayode, A. A., Badamasi, H., & Olusola, J. A. (2023). A Review on nanomaterial as photocatalysts for degradation of organic pollutants. *Journal of Fluorescence*. doi:10.1007/s10895-023-03332-x
- Hu, L., Yuan, H., Zou, L., Chen, F., & Hu, X. (2015). Adsorption and visible light-driven photocatalytic degradation of Rhodamine B in aqueous solutions by Ag@AgBr/SBA-15. *Applied Surface Science*, 355, 706-715. doi:https://doi.org/10.1016/j.apsusc.2015.04.166
- Issarapanacheewin, S., Wetchakun, K., Phanichphant, S., Kangwansupamonkon, W., & Wetchakun, N. (2016). Photodegradation of organic dyes by CeO₂/Bi₂WO₆ nanocomposite and its physicochemical properties investigation. *Ceramics International*, 42(14), 16007-16016. doi:https://doi.org/10.1016/j.ceramint.2016.07.108

- Kurian, M. (2020). Cerium oxide based materials for water treatment – A review. *Journal of Environmental Chemical Engineering*, 8(5), 104439. doi:<https://doi.org/10.1016/j.jece.2020.104439>
- Kusmierek, E. (2020). A CeO₂ Semiconductor as a photocatalytic and photoelectrocatalytic material for the remediation of pollutants in industrial wastewater: A Review. *Catalysts*, 10(12), 1435. Retrieved from <https://www.mdpi.com/2073-4344/10/12/1435>
- Linghu, X., Shu, Y., Liu, L., Zhao, Y., Zhang, J., Chen, Z., Shan, D., & Wang, B. (2023). Hydro/solvothermally synthesized bismuth tungstate nanocatalysts for enhanced photocatalytic degradation of dyes, antibiotics, and bacteria in wastewater: A review. *Journal of Water Process Engineering*, 54, 103994. doi:<https://doi.org/10.1016/j.jwpe.2023.103994>
- Ma, D., Yi, H., Lai, C., Liu, X., Huo, X., An, Z., Li, L., Fu, Y., Li, B., Zhang, B., Qin, L., Liu, S., & Yang, L. (2021). Critical review of advanced oxidation processes in organic wastewater treatment. *Chemosphere*, 275, 130104. doi:<https://doi.org/10.1016/j.chemosphere.2021.130104>
- Ma, J., Xu, N., Luo, Y., Liu, Q., & Pu, Y. (2023). Defect generation and morphology transformation mechanism of CeO₂ particles prepared by molten salt method. *Ceramics International*, 49(3), 4929-4943. doi:<https://doi.org/10.1016/j.ceramint.2022.10.007>
- Ma, R., Zhang, S., Wen, T., Gu, P., Li, L., Zhao, G., Niu, F., Huang, Q., Tang, Z., & Wang, X. (2019). A critical review on visible-light-response CeO₂-based photocatalysts with enhanced photooxidation of organic pollutants. *Catalysis Today*, 335, 20-30. doi:<https://doi.org/10.1016/j.cattod.2018.11.016>
- Mallesappa, J., Nagabhushana, H., Prasad, B. D., Sharma, S. C., Vidya, Y. S., & Anantharaju, K. S. (2016). Structural, photoluminescence and thermoluminescence properties of CeO₂ nanoparticles. *Optik*, 127(2), 855-861. doi:<https://doi.org/10.1016/j.ijleo.2015.10.114>
- Nadjia, L., Abdelkader, E., Naceur, B., & Ahmed, B. (2018). CeO₂ nanoscale particles: Synthesis, characterization and photocatalytic activity under UVA light irradiation. *Journal of Rare Earths*, 36(6), 575-587. doi:<https://doi.org/10.1016/j.jre.2018.01.004>
- Pansambal, S., Oza, R., Borgave, S., Chauhan, A., Bardapurkar, P., Vyas, S., & Ghotekar, S. (2022). Bioengineered cerium oxide (CeO₂) nanoparticles and their diverse applications: a review. *Applied Nanoscience*. doi:10.1007/s13204-022-02574-8
- Ramadan, R., & El-Masry, M. M. (2021). Comparative study between CeO₂/ZnO and CeO₂/SiO₂ nanocomposites for (Cr6+) heavy metal removal. *Applied Physics A*, 127(11), 876. doi:10.1007/s00339-021-05037-z
- Scherrer, P. (1918). Estimation of the size and internal structure of colloidal particles by means of röntgen. *Nachrichten von der Gesellschaft der Wissenschaften zu Göttingen*, 2, 96–100.
- Seeharaj, P., Kongmun, P., Paipod, P., Prakobmit, S., Sriwong, C., Kim-Lohsoontorn, P., & Vittayakorn, N. (2019). Ultrasonically-assisted surface modified TiO₂/rGO/CeO₂ heterojunction photocatalysts for conversion of CO₂ to methanol and ethanol. *Ultrasonics Sonochemistry*, 58, 104657. doi:<https://doi.org/10.1016/j.ultsonch.2019.104657>
- Sharma, J., Sharma, S., & Soni, V. (2021). Classification and impact of synthetic textile dyes on Aquatic Flora: A review. *Regional Studies in Marine Science*, 45, 101802. doi:<https://doi.org/10.1016/j.rsma.2021.101802>
- Sing, K. S. W. (1985). Reporting physisorption data for gas/solid systems with special reference to the determination of surface area and porosity (Recommendations 1984). In *Pure and Applied Chemistry* (Vol. 57, pp. 603).
- Solayman, H. M., Hossen, M. A., Abd Aziz, A., Yahya, N. Y., Leong, K. H., Sim, L. C., Monir, M.U., & Zoh, K.-D. (2023). Performance evaluation of dye wastewater treatment technologies: A review. *Journal of Environmental Chemical Engineering*, 11(3), 109610. doi:<https://doi.org/10.1016/j.jece.2023.109610>
- Tran, D. P. H., Pham, M.-T., Bui, X.-T., Wang, Y.-F., & You, S.-J. (2022). CeO₂ as a photocatalytic material for CO₂ conversion: A review. *Solar Energy*, 240, 443-466. doi:<https://doi.org/10.1016/j.solener.2022.04.051>
- Turkten, N. (2022). A novel low-cost photocatalyst: Preparation, characterization, and photocatalytic properties of CeO₂-diatomite composites. *Water*, 14(21), 3373. Retrieved from <https://www.mdpi.com/2073-4441/14/21/3373>
- Vivek, S., Arunkumar, P., & Babu, K. S. (2016). In situ generated nickel on cerium oxide nanoparticle for efficient catalytic reduction of 4-nitrophenol. *RSC Advances*, 6(51), 45947-45956. doi:10.1039/C6RA04120E

Wu, H., Sun, Q., Chen, J., Wang, G.-Y., Wang, D., Zeng, X.-F., & Wang, J.-X. (2021). Citric acid-assisted ultrasmall CeO₂ nanoparticles for efficient photocatalytic degradation of glyphosate. *Chemical Engineering Journal*, 425, 130640. doi:<https://doi.org/10.1016/j.cej.2021.130640>

Xie, L., Ren, Z., Zhu, P., Xu, J., Luo, D., & Lin, J. (2021). A novel CeO₂-TiO₂/PANI/NiFe₂O₄ magnetic photocatalyst: Preparation, characterization and photodegradation of tetracycline hydrochloride under visible light. *Journal of Solid State Chemistry*, 300, 122208. doi:<https://doi.org/10.1016/j.jssc.2021.122208>